molbank

MDPI

Communication

Ethyl 5-Formyl-1-(pyridin-3-yl)-1*H*-1,2,3-triazole-4-carboxylate: Synthesis, Crystal Structure, Hirshfeld Surface Analysis, and DFT Calculation

Nazariy T. Pokhodylo [1], Yuriy I. Slyvka [1], Evgeny A. Goreshnik [2] and Mykola D. Obushak [1,*]

[1] Faculty of Chemistry, Ivan Franko National University of Lviv, Kyryla i Mefodiya, 6, 79005 Lviv, Ukraine; nazariy.pokhodylo@lnu.edu.ua (N.T.P.); yurii.slyvka@lnu.edu.ua (Y.I.S.)
[2] Department of Inorganic Chemistry and Technology, Jozef Stefan Institute, Jamova 39, SI-1000 Ljubljana, Slovenia; evgeny.goreshnik@ijs.si
* Correspondence: mykola.obushak@lnu.edu.ua

Abstract: For the first time, 5-formyl-1-(pyridin-3-yl)-1*H*-1,2,3-triazole-4-carboxylate was synthesized via a two-step scheme. The molecular structure of the compound was determined by a single-crystal X-ray diffraction analysis. The Hirshfeld surface analysis was used to study various intermolecular interactions. The crystalline structure is marked by the presence of three types of π-interactions ($n\rightarrow\pi^*$, lp$\cdots\pi$, and $\pi\cdots\pi$) between the -C(H)=O group and triazole rings. The compound is a versatile polyfunctional building block for construction of annulated 1,2,3-triazoles.

Keywords: 5-formyl-1-(pyridin-3-yl)-1*H*-1,2,3-triazole-4-carboxylate; 1,2,3-triazoles; ortho-formyl acid; crystal structure; hydrogen bond; intermolecular interaction

check for updates

Citation: Pokhodylo, N.T.; Slyvka, Y.I.; Goreshnik, E.A.; Obushak, M.D. Ethyl 5-Formyl-1-(pyridin-3-yl)-1*H*-1,2,3-triazole-4-carboxylate: Synthesis, Crystal Structure, Hirshfeld Surface Analysis, and DFT Calculation. *Molbank* **2022**, *2022*, M1340. https://doi.org/10.3390/M1340

Academic Editor: Fawaz Aldabbagh

Received: 5 January 2022
Accepted: 11 February 2022
Published: 15 February 2022

Publisher's Note: MDPI stays neutral with regard to jurisdictional claims in published maps and institutional affiliations.

1. Introduction

Ortho-Formyl acids serve as useful building blocks for numerous classes of important molecules. Different electrophilicities of aldehyde and acid (ester) function groups make it possible to convert them independently for a unique variation of the structure in the molecular design of practically useful compounds. Thus, aiming for the application of ortho-formyl acids, in recent years, a number of works have been published. For example, new protocols for the synthesis of 3-difluoroalkyl phthalides [1], 3-benzylphthalides [2], 3-(1′-indolyl)-phthalides [3], and electrochemical protocol for isoindolinones [4] were developed. Syntheses of (+)-Rubellin C [5], benzo[f]pyrrolo[1, 2-*a*][1,4] diazepines [6], fluorinated isocoumarines [7], furo[2,3-*d*]pyridazines [8], furo[3,4-c]pyridines [9], 1-oxo-9*H*-thiopyrano[3,4-b]indoles [10], pyrazoloisoindoles [11], phthalazines [12] and isothiocoumarines [13] were studied. ortho-Formyl acids were used for the synthesis of biologically active compounds with anticancer potential [14]; PROTACs E3 ubiquitin ligase inhibitor [15] and MDM2 [16] degrades; STING [17] and PKM2 [18] modulators; inhibitors of Eg5 [19], SIRT1 and SIRT2 [20], 15-lipoxygenase-1 [21] and pyruvate kinase activators [22].

5-Formyl-1,2,3-triazole-4-carboxylic acids are one of the least studied triazole derivatives, although the first representative of this series was obtained in 1989 by L'Abbe, Gerrit et al. [23]. Afterwards, 5-formyl-1,2,3-triazole-4-carboxylic acids were mentioned in the synthesis of purine nucleoside analogues for treating flaviviruses diseases [24] and cyclic amine derivatives as platelet activation inhibitors [25]. In addition, 5-formyl-triazoles were used as valuable starting materials for unsymmetrically substituted bi-1,2,3-triazoles [26]. Recently, we developed a convenient synthetic protocol to ethyl 1-aryl-5-formyl-1*H*-1,2,3-triazole-4-carboxylates [27] and prepared several new [1,2,3]triazolo[4,5-*d*]pyridazin-4-ones [28] based on it. To our knowledge, 1-hetaryl-5-formyl-1,2,3-triazole-4-carboxylic acid derivatives are still unknown. Therefore, the synthesis of such derivatives is relevant for expansion of chemical space.

2. Results and Discussion

A recent program in our laboratory has been dedicated to the synthesis of polyfunctional 1-hetaryl-1,2,3-triazole systems. In this context, we have reported; on the first synthetic use of π-deficient heterocyclic azides [29,30]. It should be noted that previously, 3-azidopyridine was studied in the reaction with ethyl acetoacetate to provide ethyl 5-methyl-1-(pyridin-3-yl)-1*H*-1,2,3-triazole-4-carboxylate in the presence of sodium methoxide [31] or 1,8-diazabicyclo[5.4.0]-undec-7-ene (DBU) [32] as bases. In the current work, 3-azidopyridine **1** was examined in the reaction with ethyl 4,4-diethoxy-3-oxobutanoate **2** using K_2CO_3 as the base and DMSO as the solvent. Under the selected protocol, 1-(pyridin-3-yl)-1*H*-1,2,3-triazole-4-carboxylate **3** with 4,4-diethoxymethyl moiety in position 5 was obtained in high yield. The last one was readily converted to 5-formyltriazole-4-carboxylate **4** in quantitative yield by heating with hydrochloric acid (Scheme 1).

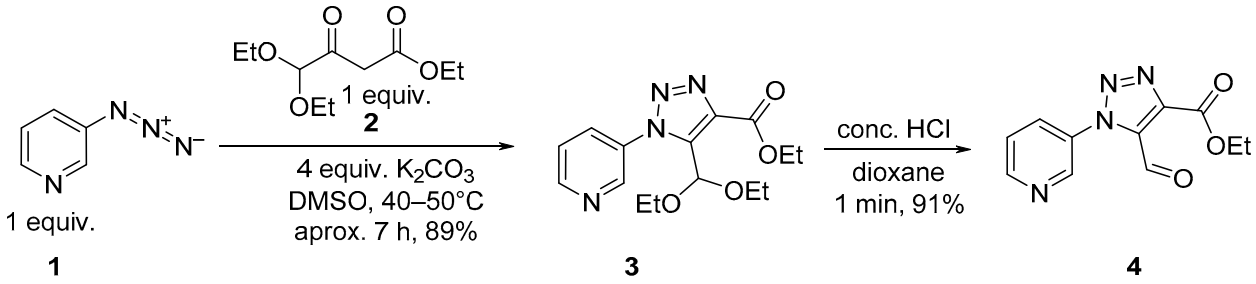

Scheme 1. Synthesis of ethyl 5-formyl-1-(pyridin-3-yl)-1*H*-1,2,3-triazole-4-carboxylate **4**.

The compound was fully characterized with NMR spectra and X-ray diffractometry. ^{1}H and ^{13}C-NMR spectra data are in good agreement with the proposed structures of products **3** and **4**. In the proton NMR spectrum of compound **3**, the non-equivalence of protons of CH_2 groups of acetal motif was observed. The CH_2 groups have appeared as a "two doublet" of quartets at 3.45 and 3.62 ppm. The acetal C-H proton is present as a singlet at 6.2 ppm. In the ^{13}C-NMR spectrum of compound **3**, the characteristic acetal carbon signal appeared at 94.75 ppm. After the cleavage of acetal (compound **4**), the characteristic aldehyde carbon signal appeared at 180.7 ppm (for more details see Supplementary Materials). What is noteworthy is that, in some related ethyl 1-aryl-5-formyl-1*H*-1,2,3-triazole-4-carboxylates studied before, the formation of stable aldehyde hydrates was found by NMR spectra [28]. However, in compound **4,** only aldehyde form is observed.

The compound **4** was crystallized in the monoclinic acentric space group *Cc*, with one triazole molecule in the asymmetric unit (Figure 1, Table 1). The triazole ring and its bound with the pyridin-3-yl ring were twisted relative to each other by 74.02(8)° because of the steric hindrance of the formyl group attached to C5. The above angle between the planes is higher than the angle between the analogous planes in ethyl 5-methyl-1-(pyridin-3-yl)-1*H*-1,2,3-triazole-4-carboxylate (50.3(3)°) [33] or between the triazole and phenyl planes in structures of 4-*t*-butyl-, 4-trimethylsilyl-, 4-trimethylgermyl-1-(4-nitrophenyl)-1,2,3-triazol-5-carbaldehydes (52.5(3)°, 62.3(2)°, 64.5(5)°, correspondingly) [34]. For comparison, in the structure of triazoles, (4-methylphenyl)[1-(pentafluorophenyl)- 5-(trifluoromethyl)-1*H*-1,2,3-triazol-4-yl]methanone, 5-cyclopropyl-*N*-(2-hydroxyethyl)-1-(4-methylphenyl)-1*H*-1,2,3-triazole-4-carboxamide, *N*-(4-chlorophenyl)-5-cyclopropyl-1-(4-methoxyphenyl)-1*H*-1,2,3-triazole-4-carboxamide, 5-methyl-1-(4-nitrophen)-1*H*-1,2,3-triazol-4-yl-phosphonate previously studied by us, the phenyl ring and the heterocyclic ring were twisted relative to each other by 62.3 (2)°, 32.75 (7)°, 87.77 (7)°, 45.35 (6)°, correspondingly [35–38].

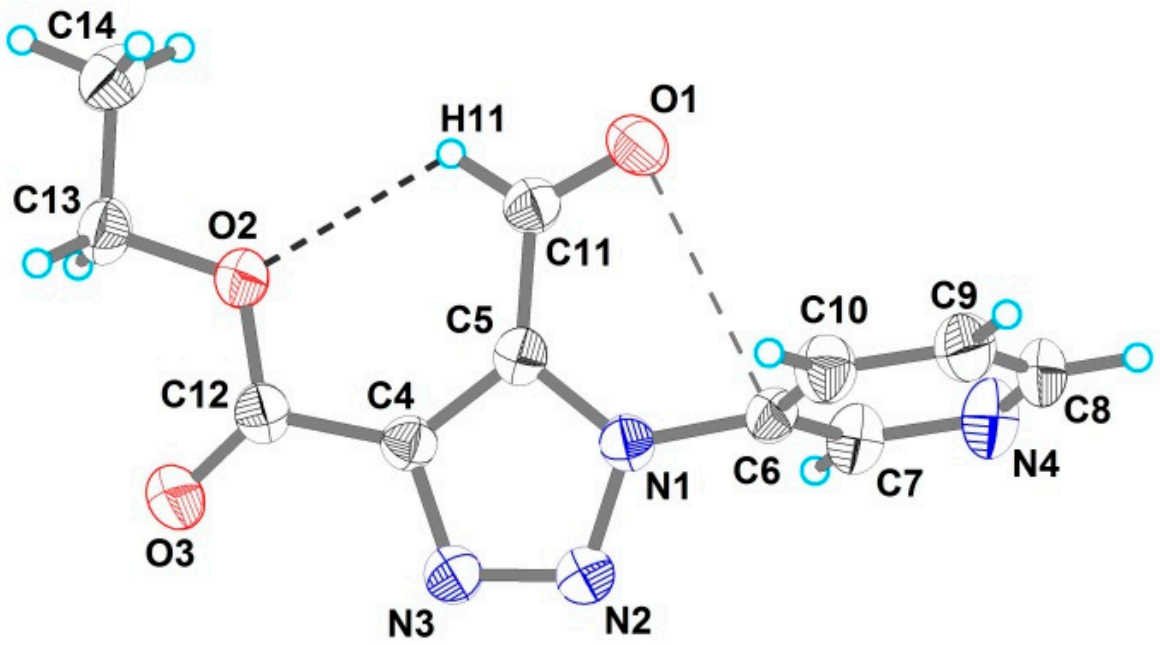

Figure 1. The molecular structure of **4** (derived from a single-crystal XRD experiment) with displacement ellipsoids drawn at the 50% probability level. Intramolecular hydrogen bond and $n\rightarrow\pi^*$ interaction are shown as dashed lines.

Table 1. Selected bond lengths (Å) and angle values (°) in the structure of **4**.

Bond	Å	Angles	°
C11–O11	1.199(3)	N1–C5–C11	124.5(2)
C5–C11	1.478(4)	O1–C11–C5	123.7(3)
N1–C6	1.444(3)	O2–C12–C4	125.0(3)
N1–N2	1.358(3)	N1–C5–C11–O1	−3.5(4)
C12–O3	1.191(3)	C5–C4–C12–O2	−3.3(4)

The carbaldehyde group in **4** is almost coplanar to the plane of the triazole ring (the N1–C5–C11–O1 torsion angle is −3.5(4)°) and its oxygen atom is oriented toward the neighboring pyridyl ring, while the aldehyde H11 atom is involved into weak intramolecular bonding with O2 atom of the ester group (Table 2). Thus, the O2 atom is involved in the intramolecular $n\rightarrow\pi^*_{Ar}$ interaction [39–41] with the aromatic system of the 1-(pyridin-3-yl) substituent (the O1–C6 bond distance is 2.952(4) Å). We should note that, in 4-*t*-butyl-, 4-trimethylsilyl-, 4-trimethylgermyl-1-(4-nitrophenyl)-1,2,3-triazol-5-carbaldehydes, the orientation of the -C(H)=O group is the opposite to that in compound **4** and corresponding torsion angles (N–C–C–O) are 168.7(3), −177.9(2), −179.5(5)°. Noteworthy, compound **4** is only the second (after 5-methyl-1-(pyridin-3-yl)-1*H*-1,2,3-triazole-4-carboxylate) known structurally studied 1-(pyridin-3-yl)-1*H*-1,2,3-triazole derivative.

Table 2. Geometry of hydrogen bonds in the structure of **4**.

Atoms Involved	Symmetry	Distances, Å			Angle, Deg
D–H···A		D–H	H···A	D···A	D–H···A
C10–H10···O1	$x, -y+2, z+0.5$	0.95	2.55	3.267(4)	132
C10–H10···N2	$x, y+1, z$	0.95	2.79	3.562(4)	139
C14–H14B···O3	$x, y+1, z$	0.98	2.67	3.592(4)	157
C8–H8···O3	$x+0.5, y+0.5$	0.95	2.69	3.617(4)	164

In absence of classical H-bonding, the structure of **4** is covered by a variety of weak intermolecular interactions (Figure 2, Table 2). Hydrogen atom H11 of the pyridin-3-yl ring is involved in C–H···O bonding with the aldehyde group O1 atom and into weak C–H···N bonding with triazole N2 atom of nearest molecules, while another pyridin-3-yl H8 atom participates in C–H···O bonding with the O3 atom of the ester group of another neighboring molecule. The H14 atom of the ethyl group is also involved in C–H···O bonding with the ester group O3 atom. The most intriguing feature of the structure of **4** is the presence of three types of π-interactions, $n \rightarrow \pi^*$ (*Type A*), lone-pair···π (lp···π) [42] (*Type B*), and π···π (*Type C*) interactions between the -C(H)=O group and triazole rings of the nearest molecules (see Figure 3). The above C–N distances are shorter than the sum of the corresponding VdW radii of C and N (3.25 Å by Bondi [43]; 3.43 Å by Alvarez [44]), the O–N distance is shorter than the sum of the corresponding VdW radii O and N (3.07 Å by Bondi [43]; 3.16 Å by Alvarez [44]).

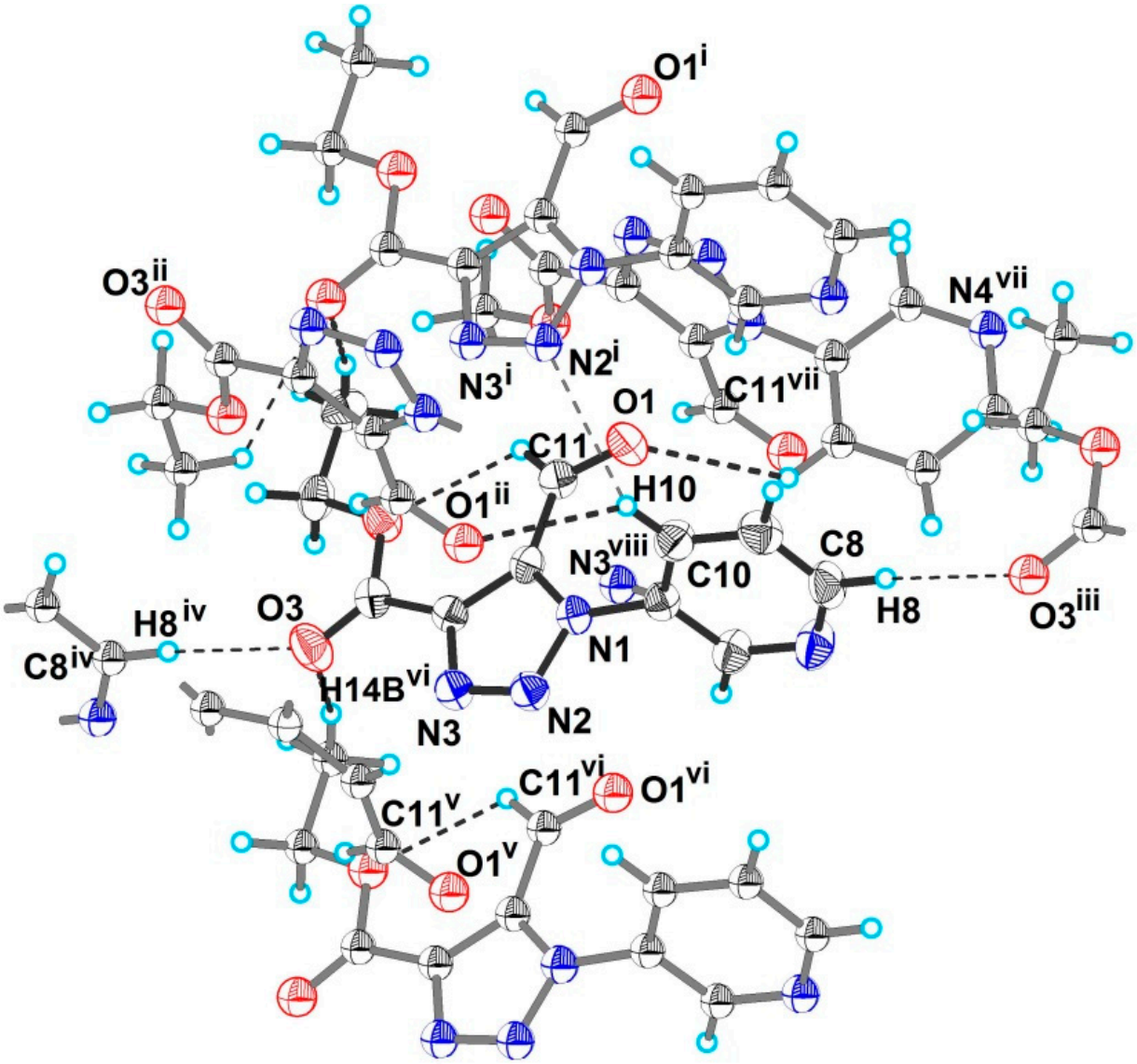

Figure 2. The hydrogen bonding of molecules in crystal structure of **4**. Hydrogen bonds are shown as dashed lines. Symmetry codes: (i) $x, y + 1, z$; (ii) $x, -y + 2, z + 0.5$; (iii) $x + 0.5, y + 0.5, z$; (iv) $x - 0.5, y - 0.5, z$; (v) $x, -y + 1, z + 0.5$; (vi) $x, y - 1, z$; (vii) $x, -y + 2, z - 0.5$, (viii) $x, -y + 1, z - 0.5$.

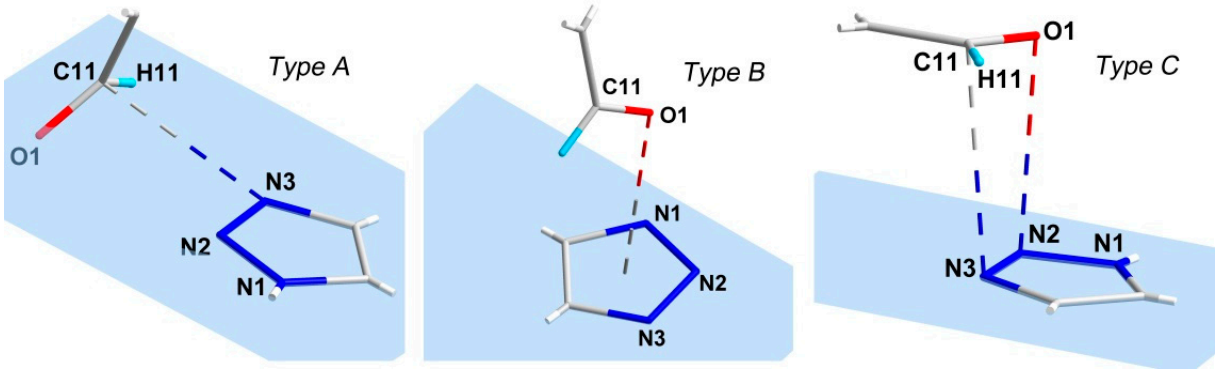

Figure 3. Three types ($n\rightarrow\pi^*$ (*Type A*, C11–N3^{viii} 3.020(4) Å; symmetry code: (viii) x, $-y+1$, $z-0.5$), lp$\cdots\pi$ (*Type B*, 3.077(4) Å, O1–N1^{vii} 3.117(4) Å; symmetry code: (vii) x, $-y+2$, $z-0.5$) and $\pi\cdots\pi$ (*Type C*, ~3.24 Å; C11–N3^{i} 3.304(4) Å; (i) x, $y+1$, z)) of π-interactions between -C(H)=O group and triazole rings in crystal structure of **4**.

The Hirshfeld surface analysis was used to analyze various intermolecular interactions in the title compound by mapping the normalized contact distance (d_{norm}) using *CrystalExplorer* (Turner et al., 2017; Spackman and Jayatilaka, 2009) [45,46]. The most prominent interactions ($n\rightarrow\pi^*$ interactions) can be seen in the Hirshfeld surface plot as the strongly red areas (Figure 4). Poorly red and white areas in the surface plot of triazole molecule correspond to the mentioned above C–H$\cdots$O and C–H$\cdots$N hydrogen bonds between neighboring molecules. The $\pi\cdots\pi$ and lp$\cdots\pi$ interactions are very weak and can be seen only as white areas. Fingerprint plots were produced to show the intermolecular surface bond distances with the regions highlighted for O$\cdots$H/H$\cdots$O and N$\cdots$H/H$\cdots$N contacts interactions (Figure 4). The contributions to the surface area for such contacts are 20.6% and 19.9%, respectively. Despite the presence of the strongly red areas in the Hirshfeld surface plot, the contribution to the surface area for $n\rightarrow\pi^*$ as well as for the $\pi\cdots\pi$ and lp$\cdots\pi$ interactions is only 11.8% in total. The contribution for H$\cdots$H contacts is 27.3%.

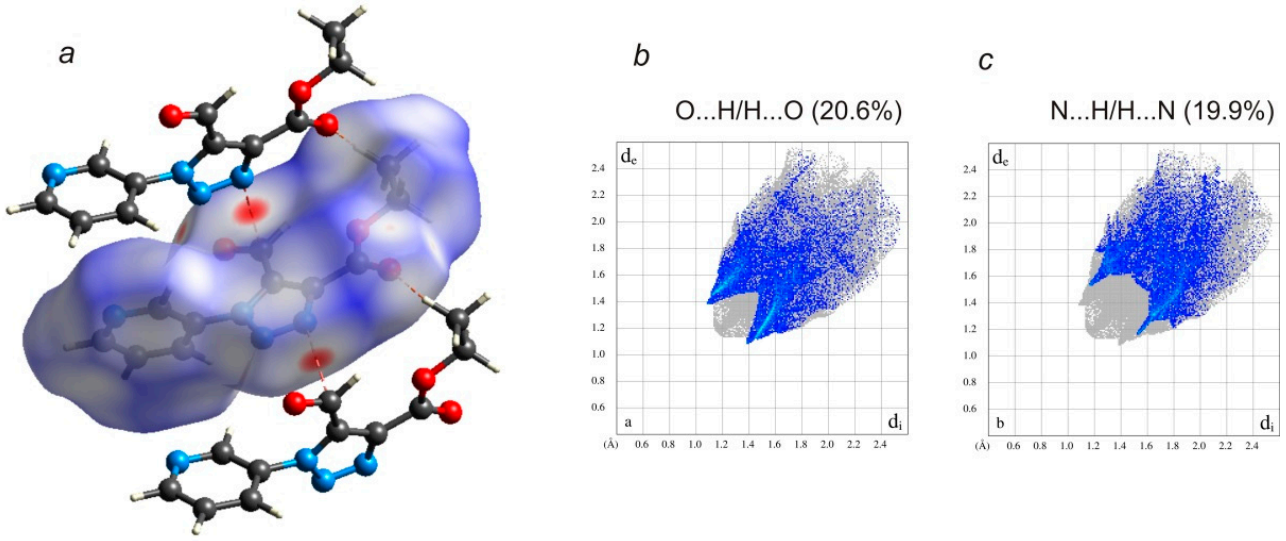

Figure 4. (**a**) Hirshfeld surface for the title molecule mapped with d_{norm} over the range -0.140 to 1.238 a.u. showing $n\rightarrow\pi^*$ and C–H$\cdots$O interactions. Fingerprint plots resolved into (**b**) O$\cdots$H/H$\cdots$O and (**c**) N$\cdots$H/H$\cdots$N contacts. Neighboring molecules associated with close contacts are also shown.

The energy framework calculations [47] discussed in this paper were performed on the DFT/B3LYP/6-31G(d, p) level of theory. All calculations were provided for the cluster of molecules within a radius of 3.8 Å, which were generated around a single fragment. The

values of interaction energy calculated between the molecules in **4** are tabulated in Table 3 and visualized in Figure 5. The cylinders in the energy framework represent the relative strengths—interaction energies are proportional to the thickness of cylinders joining the centroids of molecules.

Table 3. The intermolecular interaction energies (kJ/mol) in crystal structure of **4**.

No [a]	Symmetry Codes	*R* [b]	*E*_ele	*E*_pol	*E*_dis	*E*_rep	*E*_tot [c]
M_I	(i) $x, y + 1, z$ (vi) $x, y - 1, z$	5.35	−18.7	−4.8	−35.2	24.1	−39.1
M_{II}	(v) $x, -y + 1, z + 0.5$ (viii) $x, -y + 1, z - 0.5$	5.11	−17.9	−7.1	−32.5	21.8	−39.1
M_{III}	(ix) $x + 0.5, -y + 1.5, z + 0.5$ (x) $x - 0.5, -y + 1.5, z - 0.5$	12.25	−1.7	−0.9	−10.7	6.8	−7.6
M_{IV}	(ii) $x, -y + 2, z + 0.5$ (vii) $x, -y + 2, z - 0.5$	5.31	−10.1	−3.8	−35.9	23.5	−30.3
M_V	(iii) $x + 0.5, y + 0.5, z$; (iv) $x - 0.5, y - 0.5, z$	12.19	−3.9	−1.7	−7.9	6.0	−8.6
M_{VI}	(xi) $x + 0.5, y - 0.5, z$ (xii) $x - 0.5, y + 0.5, z$	12.19	−4.2	−1.6	−9.0	5.7	−10.0
M_{VII}	(xiii) $x + 0.5, -y + 2.5, z + 0.5$ (xiv) $x - 0.5, -y + 2.5, z - 0.5$	13.44	1.9	−0.5	−3.9	2.6	−0.2

[a] *No* is the numbering of the neighboring two molecules (M_I–M_{VII}) involved into the same interactions with the selected molecule (M). [b] *R* is the distance between molecular centroids (mean atomic position) in Å. [c] Each "energy" should be multiplied by the conversion factors $k_{ele} = 1.057$, $k_{pol} = 0.740$, $k_{dis} = 0.871$, $k_{rep} = 0.618$ to obtain the total energy (E_{tot}).

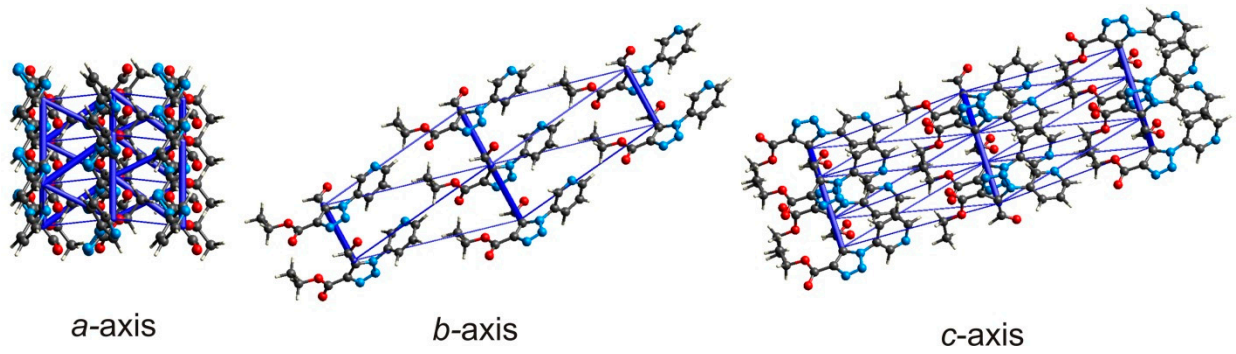

Figure 5. Energy frameworks of **4** representing the total interaction energy (blue) along the different crystallographic directions (cut-off –6.0 kJ/mol).

According to the calculation results (Figures 4 and 5, Table 3), the strongest intermolecular interactions correspond to binding of the selected molecule to the three pairs of molecules, M_I, M_{II} and M_{IV} (Figure 6). The interactions of the selected molecule with M_{II} correspond to $n \rightarrow \pi^*$ interactions and cover the total energy of −39.1 kJ/mol. The energy value of interactions with M_I (by value is the same as with M_{II}) is related to the discussed $\pi \cdots \pi$ interaction, to weak C–H···N bonding of the pyridyl H10 atom with the triazole N atom as well, as to weak C14–H14B···O3 bonding (Table 2) of the methyl group with the carboxylate O3 atom. Interactions of the main molecule with two dimers M_{IV}, which correspond to the C10–H10···O1 hydrogen bonding and lp$\cdots\pi$ interactions, cover the total energy of –30.3 kJ/mol and also with significant influence of dispersion forces. The energy value of interaction C8–H8···O3 with M_{VI} is −8.6 kJ/mol. The total energy of all interactions between the molecules in **1** is −134.9 kJ/mol.

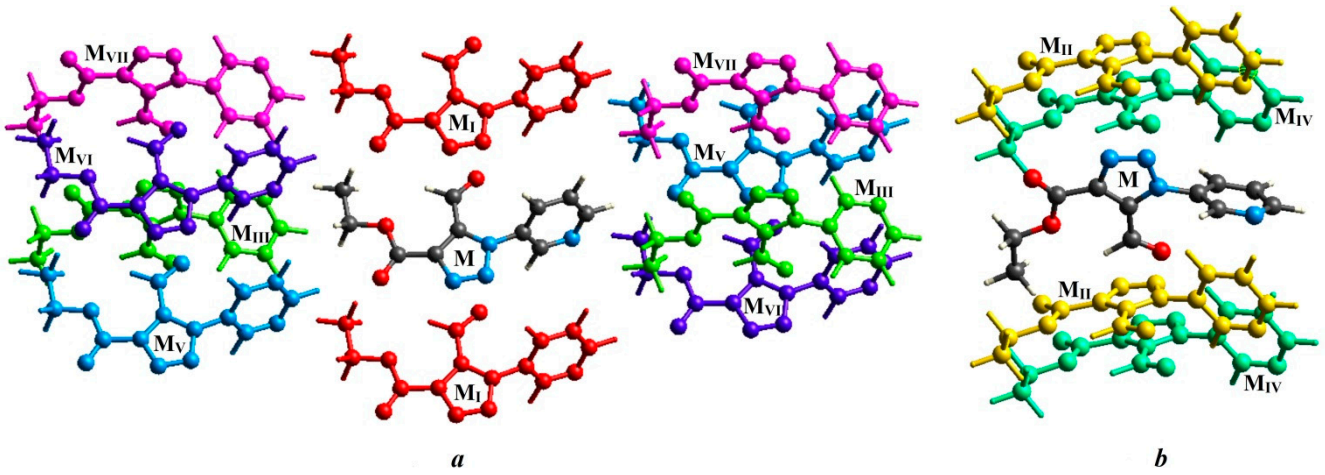

Figure 6. The principal interactions between molecules in **1** with numbering of two neighboring molecules (M_I–M_{VII}) involved in the same interactions with the selected one (M). For better perception, the molecules from the cluster are divided into two parts (**a**,**b**), represented at different crystallographic directions.

3. Experimental Section

^{1}H and ^{13}C-NMR spectra were recorded on Bruker Avance 500 (500 and 126 MHz, respectively) spectrometers in DMSO-d_6 solutions using the solvent line as internal reference. Mass spectral analyses were performed using an Agilent 1100 series LC/MSD with an API-ES/APCI mode (200 eV) instrument. Elemental analyses were accomplished using a Carlo Erba 1106 instrument. Melting points were determined on a Boetius melting point apparatus. Progress of reactions and purity of the synthesized compounds were examined by TLC on Silufol UV-254 plates, and visualization was performed using a UV lamp (254 nm). Diffraction data were collected on a Gemini+ diffractometer with Cu *Ka* radiation (λ = 1.54184 Å) and Atlas CCD detector. The 3-pyridyl azide **1** [31] and 4,4-diethoxy-3-oxobutanoate **2** [48] were prepared according to literature procedures.

3.1. Synthesis of Ethyl 5-(Diethoxymethyl)-1-(pyridin-3-yl)-1H-1,2,3-triazole-4-carboxylate 3

Anhydrous K_2CO_3 (5.53 g, 40 mmol) and ethyl 4,4-diethoxy-3-oxobutanoate **2** (2.18 g, 10 mmol) were added to a solution of 3-pyridyl azide **1** (1.2 g, 10 mmol) in DMSO (4 mL). The suspension was stirred at 40–50 °C until TLC (eluent hexane–EtOAc, v/v 5:1) indicating that all starting materials were consumed (approximately 7 h). The reaction mixture was cooled to 5 °C, diluted with H_2O (15 mL), and then extracted with CH_2Cl_2 (3 × 10 mL). The combined organic layers were concentrated under reduced pressure to afford product **3**. Yield 89%; slight yellow oil; ^{1}H-NMR (500 MHz, DMSO-d_6) δ_H 8.83 (s, 1H, H_{Py}-2), 8.76 (d, $^3J_{H,H}$ = 4.6 Hz, 1H, H_{Py}-6), 8.13–8.08 (m, 1H, H_{Py}-4), 7.64 (dd, $^3J_{H,H}$ = 8.0, 4.8 Hz, 1H, H_{Py}-5), 6.20 (s, 1H, CH), 4.39 (q, $^3J_{H,H}$ = 7.0 Hz, 2H, CH_2), 3.62 (dq, $^{2,3}J_{H,H}$ = 14.0, 7.0 Hz, 2H, CH_2), 3.45 (dq, $^{2,3}J_{H,H}$ = 14.0, 7.0 Hz, 2H, CH_2), 1.35 (t, $^3J_{H,H}$ = 7.1 Hz, 3H, CH_3), 0.96 (t, $^3J_{H,H}$ = 7.0 Hz, 6H, 2xCH_3); ^{13}C-NMR (126 MHz, DMSO-d_6) δ_C 160.8 (O=C-O), 151.2 (CH_{Py}-6), 146.8 (CH_{Py}-2), 139.8 ($C_{Triazole}$-5), 137.1 ($C_{Triazole}$-4), 134.3 (C_{Py}-3), 134.2 (CH_{Py}-4), 124.1 (CH_{Py}-5), 94.8 (CH), 64.1 (2xCH_2O), 61.7 (CH_2O), 15.1 (2xCH_3), 14.5 (CH_3); MS (CI, 200 eV), m/z (I_{rel}, %): 321 (M^+ + 1). Found, %: C, 56.21; H, 6.27; N, 17.43. $C_{15}H_{20}N_4O_4$ (320.3490). Calculated, %: C, 56.24; H, 6.29; N, 17.49.

3.2. Synthesis of Ethyl 5-Formyl-1-(pyridin-3-yl)-1H-1,2,3-triazole-4-carboxylate 4

Concentrated HCl (0.5 mL) was added to a solution of compound **3** 640 mg (2 mmol) in 1,4-dioxane (5 mL). The mixture was heated under reflux for 1 min and cooled to 0 °C. Anhydrous K_2CO_3 (approximately 400 mg) was slowly added to neutrality. The mixture was concentrated under reduced pressure. The residue was extracted with boiling hexane

(3 × 15 mL) for a short time and then the hexane solution was quickly separated by decantation. Concentration and cooling of the hexane extracts gave crystals of the product. Yield 91%; white solid; mp 112–114 °C; ^{1}H-NMR (500 MHz, DMSO-d_6) δ_H 10.26 (s, 1H, CHO), 8.81 (s, 1H, H_{Py}-2), 8.78 (d, $^{3}J_{H,H}$ = 4.7 Hz, 1H, H_{Py}-6), 8.09 (d, $^{3}J_{H,H}$ = 8.1 Hz, 1H, H_{Py}-4), 7.65 (dd, $^{3}J_{H,H}$ = 7.6, 5.2 Hz, 1H, H_{Py}-5), 4.43 (q, $^{3}J_{H,H}$ = 6.9 Hz, 2H, CH_2), 1.34 (t, $^{3}J_{H,H}$ = 7.0 Hz, 3H, CH_3); ^{13}C-NMR (126 MHz, DMSO-d_6) δ_C 180.7 (O=C-H), 160.1 (O=C-O), 151.8 (CH_{Py}-6), 146.7 (CH_{Py}-2), 141.8 ($C_{Triazole}$-4), 136.0 ($C_{Triazole}$-5), 134.2 (CH_{Py}-4), 133.4 (C_{Py}-3), 124.5 (CH_{Py}-5), 62.4 (CH_2O), 14.5 (CH_3); MS (CI, 200 eV), m/z (I_{rel}, %): 247 (M^+ + 1). Found, %: C, 53.70; H, 4.07; N, 22.70. $C_{11}H_{10}N_4O_3$ (246,2260). Calculated, %: C, 53.66; H, 4.09; N, 22.75. Single-crystal X-ray diffraction: monoclinic crystal system, space group *Cc*, *Z* = 4, unit cell dimensions: a = 23.7940(11), b = 5.3470(3), c = 8.9367(5) Å, β = 96.216(4)°, V = 1130.30(10) Å^3 at 200 K; ρ_{calcd} = 1.447 g/cm^3, $R[F^2 > 2\sigma(F^2)]$ = 0.0332 for 2015 reflections and $wR(F^2)$ = 0.0904 for all 2090 reflections, flack parameter is 0.02(17). Data were deposited at the Cambridge Crystallographic Data Centre, as CCDC 2130866 contains the supplementary crystallographic data for this paper. These data can be obtained free of charge from the Cambridge Crystallographic Data Centre via https://www.ccdc.cam.ac.uk/structures/ (accessed on 3 February 2022).

Supplementary Materials: The following supporting information, containing NMR spectra of new synthesized compounds **3**, **4**, can be downloaded online.

Author Contributions: N.T.P. designed the experiments, performed syntheses, obtained the NMR spectra, and wrote the draft; Y.I.S. and E.A.G. collected the X-ray data and solved the structure; M.D.O. analyzed the data and finalized the draft. All authors have read and agreed to the published version of the manuscript.

Funding: The authors thank the Ministry of Education and Science of Ukraine for financial support of this project (grant no. 0121U107777).

Institutional Review Board Statement: Not applicable.

Informed Consent Statement: Not applicable.

Data Availability Statement: The X-ray data were deposited at CCDC, as stated above, and all spectroscopic data are in the Supplementary Materials.

Conflicts of Interest: The authors declare no conflict of interest.

References

1. Liu, S.; Li, Y.; Wang, F.; Ma, C.; Yang, G.; Yang, J.; Ren, J. p-Toluenesulfonic acid-catalyzed reaction of phthalaldehydic acids with difluoroenoxysilanes: Access to 3-difluoroalkyl phthalides. *Synthesis* **2021**, *54*, 161–170. [CrossRef]
2. Ibrahimi, M.; Khoumeri, O.; Abderrahim, R.; Terme, T.; Vanelle, P. Synthesis of 3-benzylphthalide derivatives by using a TDAE strategy. *Synlett* **2021**, *32*, 283–286. [CrossRef]
3. Yuan, S.; Zhang, D.-Q.; Zhang, J.-Y.; Yu, B.; Liu, H.-M. palladium-catalyzed ligand-free double cyclization reactions for the synthesis of 3-(1′-indolyl)-phthalides. *Org. Lett.* **2020**, *22*, 814–817. [CrossRef]
4. Zou, Z.; Cai, G.; Chen, W.; Zou, C.; Li, Y.; Wu, H.; Chen, L.; Hu, J.; Li, Y.; Huang, Y. Metal-free cascade formation of intermolecular c-n bonds accessing substituted isoindolinones under cathodic reduction. *J. Org. Chem.* **2021**, *86*, 15777–15784. [CrossRef] [PubMed]
5. Gartman, J.A.; Tambar, U.K. Total synthesis of (+)-Rubellin C. *Org. Lett.* **2020**, *22*, 9145–9150. [CrossRef]
6. Gao, Z.; Qian, J.; Yang, H.; Zhang, J.; Jiang, G. Bronsted acid catalyzed cyclization of inert N-substituted pyrroles to benzo[f]pyrrolo[1,2-*a*][1,4]diazepines. *Synlett* **2021**, *32*, 930–934. [CrossRef]
7. Yata, T.; Nishimoto, Y.; Chiba, K.; Yasuda, M. Indium-catalyzed C-F bond transformation through oxymetalation/β-fluorine elimination to access fluorinated isocoumarins. *Chem. Eur. J.* **2021**, *27*, 8288–8294. [CrossRef]
8. Marangoni, M.A.; Moraes, P.A.; Camargo, A.F.; Bonacorso, H.G.; Martins, M.A.P.; Zanatta, N. Synthesis of a novel 1,4-dicarbonyl scaffold-ethyl 3-formyl-4,5-dihydrofuran-2-carboxylate-and its application to the synthesis of pyridazines. *Synthesis* **2020**, *52*, 2528–2534. [CrossRef]
9. Fedoseev, S.V.; Belikov, M.Y.; Ershov, O.V. Synthesis of 3-(dialkylamino)-4-halofuro[3,4-c]pyridin-1(3H)-ones. *Rus. J. Org. Chem.* **2020**, *56*, 49–52. [CrossRef]
10. Kryshchyshyn-Dylevych, A.; Garazd, M.; Karkhut, A.; Polovkovych, S.; Lesyk, R. Synthesis and anticancer activity evaluation of 3-(4-oxo-2-thioxothiazolidin-5-yl)-1*H*-indole-carboxylic acids derivatives. *Synth. Commun.* **2020**, *50*, 2830–2838. [CrossRef]

11. Wang, X.; Huang, D.; Wang, K.-H.; Su, Y.; Hu, Y. Tin powder-promoted cascade condensation/allylation/lactamization: Synthesis of isoindolinones and pyrazoloisoindol-8-ones. *J. Org. Chem.* **2019**, *84*, 6946–6961. [CrossRef] [PubMed]
12. Lu, B.; Xie, Z.; Lu, J.; Liu, J.; Cui, S.; Ma, Y.; Hu, X.; Liu, Y.; Zhong, K. Highly atom-economic, catalyst-free, and solvent-free synthesis of phthalazinones. *ACS Sustain. Chem. Eng.* **2019**, *7*, 134–138. [CrossRef]
13. Pokhodylo, N.T.; Matiychuk, V.S.; Obushak, M.D. Synthesis of isothiocoumarin derivatives. *Chem. Heterocycl. Compd.* **2010**, *46*, 140–145. [CrossRef]
14. Kryshchyshyn-Dylevych, A.; Radko, L.; Finiuk, N.; Garazd, M.; Kashchak, N.; Posyniak, A.; Niemczuk, K.; Stoika, R.; Lesyk, R. Synthesis of novel indole-thiazolidinone hybrid structures as promising scaffold. *Bioorg. Med. Chem.* **2021**, *50*, 116453. [CrossRef] [PubMed]
15. Yang, F.; Yu, N.; Chi, J.; Jia, M.; He, W.; He, F.; Tao, W.; Bai, C. Fused Imide Derivatives as Protein Degradation Targeted Chimera Inhibitors and Their Preparation, Pharmaceutical Compositions and Use in the Treatment of Diseases. Patent WO2021143816 22 July 2021.
16. Wang, B.; Liu, J.; Tandon, I.; Wu, S.; Teng, P.; Liao, J.; Tang, W. Development of MDM2 degraders based on ligands derived from Ugi reactions: Lessons and Discoveries. *Eur. J. Med. Chem.* **2021**, *219*, 113425. [CrossRef]
17. Morrow, B.J.; Hubert, J.G.; Dennis, M.L.; Cuzzupe, A.N.; Stupple, P.A. Benzothiophene, Thienopyridine and Thienopyrimidine Derivatives for the Modulation of STING and their Preparation. Patent WO2021009362 20 January 2021.
18. Liu, T.; Sui, Z.; Ji, J. Preparation of thieno[3,2-b]pyrrole[3,2-d]pyridazinone Derivatives and Their Use as PKM2 Modulators for the Treatment of Cancer, Obesity and Diabetes-Related Disorders. Patent WO2020167976 12 February 2020.
19. Jiang, X.-Q.; Chen, S.-Q.; Liu, Y.-F.; Pan, X.-G.; Chen, D.; Wang, S.-F. Solvothermal synthesis of multiple dihydropyrimidinones at a time as inhibitors of Eg5. *Molecules* **2021**, *26*, 1925. [CrossRef]
20. Manjula, R.; Gokhale, N.; Unni, S.; Deshmukh, P.; Reddyrajula, R.; Srinivas Bharath, M.M.; Dalimba, U.; Padmanabhan, B. Design, synthesis, in-vitro evaluation and molecular docking studies of novel indole derivatives as inhibitors of SIRT1 and SIRT2. *Bioorg. Chem.* **2019**, *92*, 103281. [CrossRef]
21. Guo, H.; Verhoek, I.C.; Prins, G.G.H.; van der Vlag, R.; van der Wouden, P.E.; van Merkerk, R.; Quax, W.J.; Olinga, P.; Hirsch, A.K.H.; Dekker, F.J. Novel 15-lipoxygenase-1 inhibitor protects macrophages from lipopolysaccharide-induced cytotoxicity. *J. Med. Chem.* **2019**, *62*, 4624–4637. [CrossRef] [PubMed]
22. Cianchetta, G.; Liu, T.; Padyana, A.K.; Sui, Z.; Cai, Z.; Cui, D.; Ji, J. Thiasolopyrrolopyridazines as Pyruvate Kinase Activators for Use in Treating Blood Disorders and Their Preparation. Patent WO2019035863 21 February 2019.
23. L'Abbe, G.; Dehaen, W. Synthesis and thermal rearrangement of 5-(diazomethyl)-1,2,3-triazoles. *Tetrahedron* **1988**, *44*, 461–469. [CrossRef]
24. Storer, R.; Gosselin, G.; Dukhan, D.; Leroy, F. Preparation of Purine Nucleoside Analogs for Treating Flaviv Iridae Including Hepatitis C. Patent WO2005009418 3 February 2005.
25. Kimura, T.; Tanaka, N.; Sugidachi, A.; Konosu, T. Preparation of Cyclic Amine Derivatives Having Heteroaryl Ring as Platelet Activation Inhibitors. Patent US20060270706 30 November 2006.
26. Vroemans, R.; Horsten, T.; Van Espen, M.; Dehaen, W. 5-Formyltriazoles were used as valuable starting materials for unsymmetrically substituted bi-1,2,3-triazoles. *Front. Chem.* **2020**, *8*, 00271. [CrossRef]
27. Pokhodylo, N.T.; Shyyka, O.Y.; Matiychuk, V.S.; Obushak, M.D.; Pavlyuk, V.V. A novel base-solvent controlled chemoselective azide attack on an ester group versus keto in alkyl 3- substituted 3-oxopropanoates: Mechanistic insights. *ChemistrySelect* **2017**, *2*, 5871–5876. [CrossRef]
28. Pokhodylo, N.T.; Shyyka, O.Y.; Obushak, M.D. Convenient synthetic path to ethyl 1- aryl-5-formyl-1*H*-1,2,3-triazole-4-carboxylates and 1-aryl-1,5-dihydro-4*H*-[1,2,3]triazolo[4,5-d]pyridazin-4-ones. *Chem. Heterocycl. Compd.* **2018**, *54*, 773–779. [CrossRef]
29. Pokhodylo, N.T.; Shyyka, O.Y.; Savka, R.D.; Obushak, M.D. 2-Azido-1,3,4-thiadiazoles, 2-azido-1,3-thiazoles, and aryl azides in the synthesis of 1,2,3-triazole-4-carboxylic acids and their derivatives. *Russ. J. Org. Chem.* **2018**, *54*, 1090–1099. [CrossRef]
30. Pokhodylo, N.T.; Savka, R.D.; Pidlypnyi, N.I.; Matiychuk, V.S.; Obushak, M.D. Synthesis of 2-azido-1,3-thiazoles as 1,2,3-triazole precursors. *Synth. Commun.* **2010**, *40*, 391–399. [CrossRef]
31. Kaushik, R.; Kushwaha, K.; Chand, M.; Vashist, M.; Jain, S.C. Design and synthesis of 2, 5-disubstituted-1, 3, 4-oxadiazole hybrids bearing pyridine and 1, 2, 3-triazole pharmacophores. *J. Heterocycl. Chem.* **2017**, *54*, 042–1047. [CrossRef]
32. Pacifico, R.; Destro, D.; Gillick-Healy, M.W.; Kelly, B.G.; Adamo, M.F. Preparation of acidic 5-hydroxy-1, 2, 3-triazoles via the cycloaddition of aryl azides with β-ketoesters. *J. Org. Chem.* **2021**, *86*, 11354–11360. [CrossRef] [PubMed]
33. Brito, I.; Kesternich, V.; Pérez-Fehrmann, M.; Araneda, C.; Cárdenas, A. Crystal structure of ethyl 5-methyl-1-(pyridin-3-yl)-1*H*-1,2,3-triazole-4-carboxylate, C11H12N4O2. *Zeitschrift für Krist.-New Cryst. Struct.* **2017**, *232*, 1011–1012. [CrossRef]
34. Piterskaya, Y.L.; Khramchikhin, A.V.; Stadnichuk, M.D. Cycloaddition of organic azides to α,β-acetylenic aldimines. *Zh. Obshch. Khim.* **1996**, *66*, 1187–1188. (In Russian)
35. Pokhodylo, N.T.; Slyvk, Y.; Goreshnik, E.; Lytvyn, R. Synthesis, crystal structure and Hirshfeld surface analysis of (4-methylphenyl)[1-(pentafluorophenyl)-5-(trifluoromethyl)-1*H*-1,2,3-triazol-4-yl]methanone. *Acta Crystallogr. E.* **2021**, *77*, 1067–1071. [CrossRef] [PubMed]
36. Pokhodylo, N.T.; Slyvka, Y.; Pavlyuk, V. Synthesis, crystal structure and Hirshfeld surface analysis of 5-cyclopropyl-N-(2-hydroxyethyl)-1-(4-methylphenyl)-1*H*-1,2,3-Triazole-4-carboxamide. *Acta Crystallogr. E.* **2021**, *77*, 1043–1047. [CrossRef]

37. Pokhodylo, N.; Slyvka, Y.; Pavlyuk, V. Synthesis, crystal structure and Hirshfeld surface analysis of N-(4-chlorophenyl)-5-cyclopropyl-1-(4-methoxyphenyl)-1*H*-1,2,3-triazole-4-carboxamide. *Acta Crystallogr. E.* **2020**, *76*, 756–760. [CrossRef]
38. Pokhodylo, N.T.; Shyyka, O.Y.; Goreshnik, E.A.; Obushak, M.D. 4-Phosphonated or 4-Free 1,2,3-Triazoles: What Controls the Dimroth Reaction of Arylazides with 2-Oxopropylphosphonates? *ChemistrySelect* **2020**, *5*, 260–264. [CrossRef]
39. Bartlett, G.J.; Newberry, R.W.; VanVeller, B.; Raines, R.T.; Woolfson, D.N. Interplay of Hydrogen Bonds and n $\rightarrow\pi^*$ Interactions in Proteins. *J. Am. Chem. Soc.* **2013**, *135*, 18682–18688. [CrossRef]
40. Newberry, R.W.; Raines, R.T. The n $\rightarrow\pi^*$ Interaction. *Acc. Chem. Res.* **2017**, *50*, 1838–1846. [CrossRef]
41. Gorske, B.C.; Bastian, B.L.; Geske, G.D.; Blackwell, H.E. Local and Tunable n$\rightarrow\pi^*$ Interactions Regulate Amide Isomerism in the Peptoid Backbone. *J. Am. Chem. Soc.* **2007**, *129*, 8928–8929. [CrossRef] [PubMed]
42. Das, A.; Choudhury, S.R.; Estarellas, C.; Dey, B.; Frontera, A.; Hemming, J.; Helliwell, M.; Gamez, P.; Mukhopadhyay, S. Supramolecular assemblies involving anion–π and lone pair–π interactions: Experimental observation and theoretical analysis. *CrystEngComm* **2011**, *13*, 4519. [CrossRef]
43. Bondi, A.V. van der Waals volumes and radii. *J. Phys. Chem.* **1964**, *68*, 441–451. [CrossRef]
44. Alvarez, S. A cartography of the van der Waals territories. *Dalton Trans.* **2013**, *42*, 8617–8636. [CrossRef]
45. Turner, M.J.; Mckinnon, J.J.; Wolff, S.K.; Grimwood, D.J.; Spackman, P.R.; Jayatilaka, D.; Spackman, M.A. CrystalExplorer17. The University of Western Australia. 2017. Available online: http://hirshfeldsurface.net (accessed on 3 February 2022).
46. Spackman, M.A.; Jayatilaka, D. Hirshfeld surface analysis. *CrystEngComm* **2009**, *11*, 19–32. [CrossRef]
47. Turner, M.J.; Thomas, S.P.; Shi, M.W.; Jayatilaka, D.; Spackman, M.A. Energy frameworks: Insights into interaction anisotropy and the mechanical properties of molecular crystals. *Chem. Commun.* **2015**, *51*, 3735–3738. [CrossRef]
48. Priebbenow, D.L.; Zou, L.H.; Becker, P.; Bolm, C. The Disubstitution of Acetals to Prepare δ,δ-Bis (aryl) β-Keto Esters. *Eur. J. Org. Chem.* **2013**, *2013*, 3965–3969. [CrossRef]